文章编号 2095-1531(2021)02-0418-13

Enhanced dye-sensitized up-conversion luminescence of neodymium-sensitized multi-shell nanostructures

WANG Dan[1,2,3], XUE Bin[1,3], TU Lang-ping[3], ZHANG You-lin[3], SONG Jun[1*], QU Jun-le[1], KONG Xiang-gui[3*]

(1. *Key Laboratory of Optoelectronic Devices and Systems of the Ministry of Education/Guangdong Province, College of Physics and Optoelectronic Engineering, Shenzhen University, Shenzhen* 518060, *China*;
2. *College of Information Engineering, Shenzhen University, Shenzhen* 518060, *China*;
3. *State Key Laboratory of Luminescence and Applications, Changchun Institute of Optics, Fine Mechanics and Physics, Chinese Academy of Sciences, Changchun* 130033, *China*)

* *Corresponding author, E-mail: songjun@szu.edu.cn; xgkong*14*@ciomp.ac.cn*

Abstract: Lanthanide-ion-doped upconversion luminescence is limited by the small absorption cross-section and narrow absorption band of lanthanide ions, which results in weak luminescence. Recently, a dye-sensitized method has proven to be an effective strategy of increasing upconversion luminescence. However, simply attaching dye molecules to nanoparticles with classic Yb-doped nanostructures cannot effectively activate the sensitizing ability of the dye molecules. In response to this problem, we designed Nd-sensitized core/shell/shell ($NaYF_4$:Yb/Er (20/2%)@ $NaYF_4$:Yb (10 %)@ $NaYF_4$:Nd (80 %)) nanostructures, compared with the classic IR-806 sensitized $NaYF_4$:Yb/Er nanostructure, their upconversion luminescence (500 to 700 nm) was approximately enhanced by a factor of 38. Through analysis of the nanostructure's emission and luminescence lifetime data, the enhancement was confirmed by the effective overlap of Nd absorption with the emission of near-infrared dye molecules and the protective effects of the shell structure on the luminescent center (the lifetime of Er ($^4S_{3/2}\rightarrow{}^4I_{15/2}$) was increased by 1.7 times). In addition, we found that the doping Yb^{3+} in the outermost layer will decrease the dye-sensitized luminescence intensity. Furthermore, this Nd-sensitized core/shell/shell structure also achieved enhancement in the sensitized upconversion luminescence of the luminescence centers of Ho and Tm, which establishes a foundation for enhanced dye-sensitized upconversion luminescence.

Key words: upconversion luminescence; dye-sensitized; lanthanide ion; nanoparticles

---

收稿日期:2020-05-25; **修订日期**:2020-06-24

基金项目:国家重点基础研究发展计划 (No. 2018YFC0910602); 国家自然科学基金项目 (No. 61605130, No. 11604331, No. 61775145, No. 61835009); 吉林省科技厅自然科学基金项目 (No. 20180101222JC); 深圳市基础研究项目 (No. JCYJ20180305125425815)

Supported by National Key R&D Program of China (No. 2018YFC0910602); National Natural Science Foundation of China (No. 61605130, No. 11604331, No. 61775145, No. 61835009); Project of Science and Technology Agency, Jilin Province (No. 20180101222JC); Shenzhen Basic Research Project (No. JCYJ20180305125425815)

钕敏化多层壳纳米结构的增强型染料敏化上转换发光

王　丹[1,2,3], 薛　彬[1,3], 涂浪平[3], 张友林[3], 宋　军[1*], 屈军乐[1], 孔祥贵[3*]
（1. 深圳大学 物理与光电工程学院 光电子器件与系统教育部/
广东省重点实验室，广东 深圳 518060；
2. 深圳大学 信息工程学院，广东 深圳 518060；
3. 中国科学院 长春光学精密机械与物理研究所 发光学及应用
国家重点实验室，吉林 长春 130033）

摘要: 对于稀土离子掺杂的上转换发光, 由于稀土离子吸收截面小、吸收范围窄, 导致其发光强度受限。最近, 在稀土上转换纳米粒子的表面连接近红外染料分子敏化发光, 被证实是提高上转换发光强度的有效策略。然而, 将染料分子连接经典的稀土 Yb 掺杂纳米粒子, 并不能有效利用染料分子的敏化能力。针对这一问题, 本文通过高温热分解法成功制备了 Nd^{3+}敏化的核/壳/壳 ($NaYF_4$:Yb/Er (20/2%)@ $NaYF_4$:Yb (10 %)@ $NaYF_4$:Nd (80 %)) 纳米结构, 与经典的 IR-806 敏化的 $NaYF_4$:Yb/Er 纳米结构相比, IR-806 敏化的 Nd^{3+}掺杂的核/壳/壳纳米结构的上转换发光 (500~700 nm) 强度增强了约 38 倍。通过荧光光谱及荧光寿命分析证实, 上转换发光强度增强源于 Nd 的吸收与近红外染料分子的有效交叠, 以及壳层结构对发光中心的保护作用 (Er^{3+} ($^4S_{3/2}\rightarrow{}^4I_{15/2}$) 的寿命延长了 1.7 倍)。另外, 研究发现纳米壳层结构中最外层掺杂的 Yb^{3+}离子将导致染料敏化发光减弱。进一步, 这种 IR-806 敏化的 Nd 掺杂的核/壳/壳纳米结构可实现增强发光中心为 Ho 及 Tm 的上转换发光。本文研究为提高染料敏化上转换发光及应用提供了新途径。

关　键　词: 上转换发光; 稀土离子; 染料敏化; 纳米粒子
中图分类号: TP394.1; TH691.9　　**文献标志码:** A　　**doi:** 10.37188/CO.2020-0097

1　Introduction

Due to the unique electron transitions in 4f electron configuration and between 4f and 5d, rare earth ions can generate the photon radiation of various wavelengths from ultraviolet, visible light to infrared light[1-2]. The Up-Conversion NanoParticles (UCNPs) doped with rare earth ions have the characteristic of converting two or more low-energy near-infrared photons into a high-energy photon. In particular, the photon emission generated by UCNPs has the advantages such as narrow spectral band, resistance to bleaching, and low background noise[3]. This up-conversion luminescence induced by near-infrared light has been applied in many fields, such as super-resolution imaging, fluorescent labeling, photodynamic therapy, and optical anti-counterfeiting[4-8].

In spite of the above wide applications, the further practical application of the up-conversion luminescence generated by the doped rare earth ions has been limited by its low luminous intensity. How to enhance the up-conversion luminescence has always been an urgent problem to be solved in up-conversion luminescence research. In recent years, the techniques such as core-shell nanostructure[9], plasma field-enhanced luminescence[10] and dye-sensitized luminescence[11] have realized the enhancement of up-conversion luminescence intensity. In particular, the study of dye-sensitized luminescence has not only enhanced the intensity of up-conversion luminescence, but also broadened the excitation range of up-conversion luminescence. Instead of the rare earth ions with weak absorption (absorption coefficient: 0.1~10 M^{-1} cm^{-1}), near-infrared dyes (absorption coefficient: 1 000~10 000 M^{-1} cm^{-1})

have been used to absorb near-infrared light so as to realize the up-conversion luminescence enhanced by sensitization. However, the iterated integral of most of the near-infrared dye emission (800~900 nm) and the Yb absorption in the classical Yb-sensitized doping system (950~1,000 nm) is small, thus limiting the enhancement of dye-sensitized up-conversion luminescence. Furthermore, Nd/Er-ion sensitization system has been designed as the recipient of dye sensitization[12-13] to achieve more effective enhancement of dye-sensitized up-conversion luminescence. It is in recent years that Nd^{3+}-sensitized up-conversion luminescence system has been developed. Especially, its partitioned doping strategy can realize efficient up-conversion luminescence[14-16]. However, the dye-sensitized Nd-ion doping system usually adopts the optimum structural design of Nd-sensitized up-conversion luminescence. Considering that the dye will interact with rare earth luminescence system in the dye sensitization process to weaken the luminescence[17], the design and optimization of dye-sensitized Nd-doped up-conversion luminescence system will be more effectively applied in biochemical analysis, tumor diagnosis and treatment, luminescence display and other fields[18-22].

In this paper, Nd-sensitized core/shell/shell structure was designed as the recipient of enhanced dye-sensitized up-conversion luminescence. The Nd-sensitized core/shell/shell structure was successfully prepared by high-temperature thermal decomposition, and then was coupled with the dye IR-806 molecules to enhance the intensity of dye-sensitized up-conversion luminescence. The related structural characterization confirmed the successful preparation of this nanostructure. The enhancement mechanism behind it was further studied through the analysis of emission spectrum and fluorescence lifetime spectrum. Meanwhile, by optimizing the doping concentration of Yb ions in the outermost shell, the intensity of the dye-sensitized up-conversion luminescence without Yb doping proved to be the strongest.

2 Experiment

2.1 Experimental materials

The experimental materials include ytterbium chloride ($YbCl_3·6H_2O$, 99.99%), yttrium chloride ($YCl_3·6H_2O$), erbium chloride ($ErCl_3·6H_2O$), sodium hydroxide (NaOH, 98%), ammonium fluoride (NHF_4, 99.99%), IR-780 iodide (99%), 4-mercaptobenzoic acid (99%), 1-octadecene (ODE), oleylamine (90%)(OM) and oleic acid (90%)(OA), all of which were purchased from Sigma-Aldrich. According to the reference [14], $Nd(CF_3COO)_3$ was obtained through the reaction between Nd_2O_3 powder and excessive trifluoroacetic acid and then removing the remaining trifluoroacetic acid by evaporation. Ytterbium trifluoroacetate ($Yb(CF_3COO)_3$), yttrium trifluoroacetate ($Y(CF_3COO)_3$) and sodium trifluoroacetate (CF_3COONa) were purchased from GFS Chemicals. Dichloromethane, trichloromethane and dimethyl formamide (DMF) were purchased from Beijing Chemical Works. All the chemical reagents were of analysis purity.

2.2 Synthesis of up-conversion nanoparticles

The core-shell-shell up-conversion nanostructure is fabricated based on the published chemical process[14-15]. Firstly, synthesize the core structure. Dissolve $YbCl_3·6H_2O$ (0.1 mmol), $YCl_3·6H_2O$ (0.39 mmol) and $ErCl_3·6H_2O$ (0.01 mmol) in a three-mouth flask containing 3 mL OA and 7.5 mL ODE. Heat the mixture to 150 ℃ for 30 minutes, and then cool it to room temperature under the protection of argon. Then, dissolve NH_4F (2 mmol) and NaOH (1.25 mmol) into 5 mL methanol, add the mixture to the above three-mouth flask with rare earth salts, and heat it to 70 ℃ to remove methanol and then heat to 300 ℃ for 1h. Then, add 0.25 mmol $NaYF_4$:Yb (10%) active shell to ODE (synthesized by trifluoroacetate process) and then add to the above mixture for 10 min curing. Then, add 0.5 mmol $NaYF_4$:Nd (20%) active shell (synthesized by trifluoroacetate process) and cure it for 10 min. Finally, cool the solution to room temperature, centri-

fuge it with ethanol, and dissolve it into 6 mL trichloromethane. The core-shell-shell up-conversion nanostructures doped with different rare earth elements were all synthesized in the similar way.

2.3 Synthesis of IR-780 molecules

Similarly, dissolve organic IR-780 molecules (250 mg), 4-mercaptobenzoic acid (115.5 mg) and DMF (10 mL) in a 50-mL three-mouth flask under nitrogen protection according to the Ref. [11]. Then keep the mixture under nitrogen protection for 17 h. Filter the product solution with 0.45 μm PTFE and remove DMF through reduced-pressure distillation. Then dissolve the residue into 5 mL dichloromethane, filter the mixture again with 0.45 μm PTFE and precipitate it with ice ethyl ether. Finally, filter and dry the reactant under vacuum, and keep it in dark place.

2.4 Synthesis of IR-806 molecules

In the similar way as Refs. [8], [17], dissolve 1 mL IR-806 (x mg/mL, x = 0~20 mg/mL) into trichloromethane, and mix it with 1 mL β-$NaYF_4$:Yb/Er(20/2%) @ $NaYF_4$:Yb (10%)@ $NaYF_4$:Nd (20%) nanoparticles (Er^{3+}: ~1.67 mmol). Stir the entire reaction mixture for 24 h at room temperature, centrifuge it, and redisperse it into 1 mL trichloromethane. Test the up-conversion spectrum of IR 806-sensitized UCNPs under the Er^{3+} concentration of about 16 μmol.

2.5 Experimental characterization testing

Transmission Electron Microscope (TEM) was tested at 200 kV by use of Tecnai G2 F20 S-Twin electron microscopy. X-ray diffraction (XRD) test was performed on Rigaku D/Max-2000 by using Cu Kα radiation (λ=0.154 1 nm) as diffraction radius. Absorption spectrum was tested on a Maya 2000 spectrometer (Ocean Optics). The up-conversion spectrum was recorded by an externally coupled 808 nm laser on an ocean optical spectrometer (Maya2000). Energy Dispersive Spectrum (EDS) analysis was characterized by Hitachi S-4800. In the fluorescence lifetime test of up-conversion luminescence, 500 MHz TDS 3052 was used as the excitation light source, and the fluorescence lifetime data was obtained through an OPO (Sunlite 8000) and an oscilloscope.

3 Experimental results and discussion

3.1 Morphology and characterization of nanoparticles

The highly uniform Nd^{3+}-sensitized core-shell-shell ($NaYF_4$:Yb/Er (20/2%)@ $NaYF_4$:Yb (10%)@ $NaYF_4$:Nd (80%)) UCNP structure was successfully prepared through high-temperature thermal decomposition. The TEM photo showed that the UCNPs were in uniform size. As shown in Fig. 1, the average sizes of core ($NaYF_4$:Yb/Er (20/2%), denoted as "C"), core/shell ($NaYF_4$:Yb/Er (20/2%) @ $NaYF_4$:Yb(10%), denoted as "CS") and core/shell/shell ($NaYF_4$:Yb/Er (20/2%)@ $NaYF_4$:Yb (10%) @$NaYF_4$:Nd (80%)), denoted as "CSS") were 23.5 nm, 26.3 nm and 33.6 nm, respectively. This increasing size confirmed that an Yb transition layer of about 1.4 nm and a 3.7 nm Nd-sensitized nanoshell layer were gradually growing on the $NaYF_4$:Yb/Er nano-core. The Fig. 2(a) shows that the UCNPs have a classical hexagonal phase structure (JCPDS-16-0334). The EDS confirmed that Nd, Y, Yb and other rare earth elements were effectively doped into the nanoparticles (Fig. 2(b)). Furthermore, we synthesized the IR-806 molecule according to the reference method (Fig. 2(c)). As seen from the absorption diagram (Fig. 2(d)), its absorption peak shifted from 780 nm to 806 nm, which confirmed the successful synthesis of IR-806 molecule. Furthermore, the IR-806 molecules was modified to the surface of UCNPs according to the above method. As shown in Fig. 2(d), after an IR-806 molecule was modified to UCNPs, the absorption peak of the UCNPs was masked by the absorption spectrum of IR-806, thus confirming the successful modification of dye molecule to UCNPs.

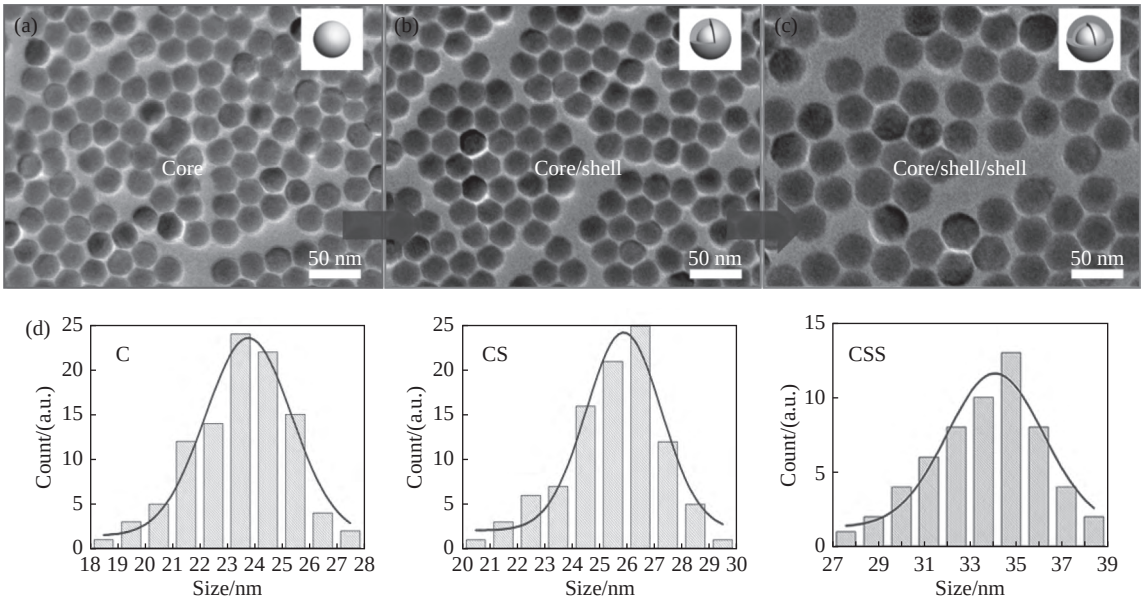

Fig. 1 TEM images of core (a), core/shell (b) and core/shell/shell (c) of up-conversion nanoparticles and their size distributions (d)

图 1 上转换纳米粒子的核(a),核/壳(b),核/壳/壳(c)电镜表征图及尺寸分布(d)

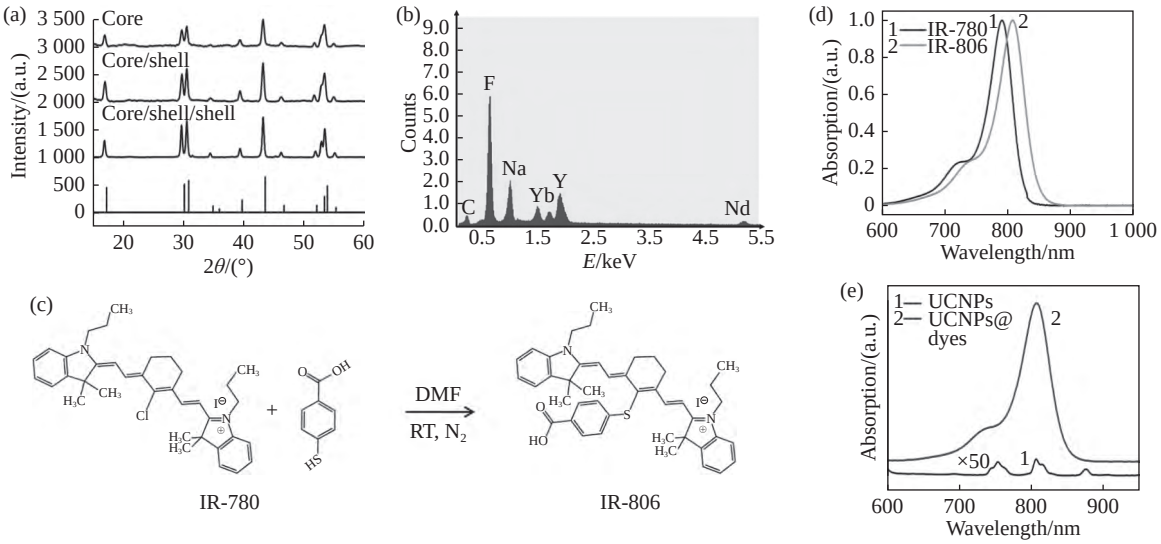

Fig. 2 (a) XRD data of C, CS and CSS of UCNPs and the β-$NaYF_4$ (JCPDS-16-0334, bottom); (b) EDS data of CSS; (c) IR-806 synthesis process; (d) absorptions of IR-780 and IR-806 before and after synthesis; (e) absorption of UCNPs and dye conjugated UCNPs after IR-806 connection

图 2 (a)上转换纳米粒子的核、核/壳、核/壳/壳 XRD 及标准卡片 β-$NaYF_4$ (JCPDS-16-0334, 底部)结果,(b)上转换 CSS 的 EDS 数据,(c)IR-806 合成过程图,(d)合成前后 IR-780 和 IR-806 的吸收,(e)连接 IR-806 之后 UCNPs 吸收和 UCNPs 本身的吸收

3.2 Confirmation and discussion of dye-sensitized enhancement mechanism

As shown in Fig. 3(a), the up-conversion luminescence intensity of the dye-sensitized CSS structure proposed in this paper is about 38 times stronger than that of the classical IR-806-sensitized $NaYF_4$:Yb/Er (20/2%) nanoparticle reported at the earliest[11]. This proves that the dye-sensitized structure has achieved the enhancement of up-conversion luminescence intensity. In addition, under the excitation of 808 nm near-infrared light, the intensities of both the up-conversion red and green light emissions of dye-sensitized CSS structure were nonlinearly dependent on excitation light power (Fig. 3

(b)). The corresponding multiphoton indexes were 1.67 (540 nm green light emission: $^4S_{13/2}\rightarrow{}^4I_{15/2}$) and 2.0 (655 nm red light emission: $^4F_{9/2}\rightarrow{}^4I_{15/2}$). Therefore, the luminescence of this structure proves to be nonlinear up-conversion luminescence.

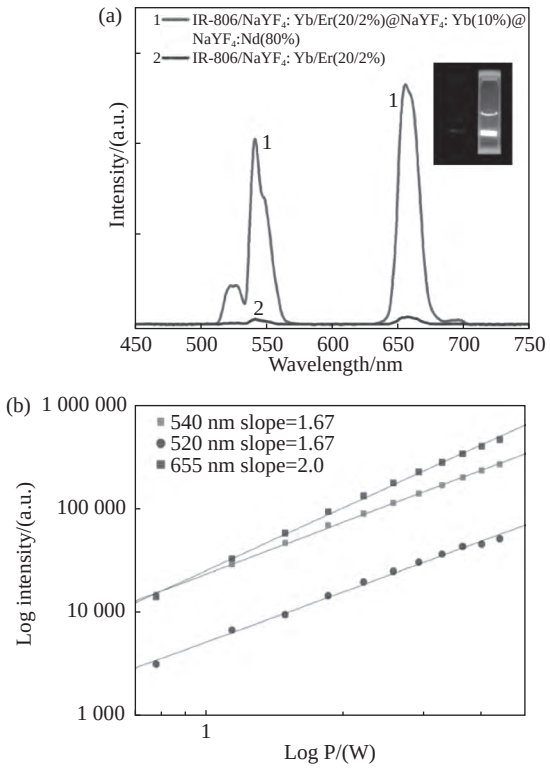

Fig. 3　(a) Up-conversion luminescence (UCL) spectra of IR-806-sensitized CSS structure and IR-806-sensitized core structure under 808 nm excitation wavelength; (b) log-log plots of the UCL intensity versus laser power for the IR-806 dye-sensitized CSS under 808 nm excitation

图 3　(a)IR-806 敏化 CSS 结构的上转换光谱及 IR-806 敏化核结构的上转换光谱, 激发波长为 808 nm, (b)808 nm 激发下的 IR-806 敏化的 CSS 结构的上转换发光强度随功率变化的 log-log 关系

According to our analysis, the outermost layer of CSS nanostructure is Nd^{3+}-doped shell, where Nd can be sensitized by IR-806 molecules efficiently due to the serious overlap between the Nd absorption and the emission of IR-806 dye molecules, as shown in Fig. 4(a) (Color online). On the other hand, the nanoshell in CSS structure can effectively protect the luminescence center. As seen from Fig. 4(b) (Color online), the luminescence lifetime of Er (253 μs) in the dye-sensitized CSS structure was significantly longer than that of Er in the dye-sensitized core nanoparticle (146 μs) or core nanoparticle (169 μs). In other words, the luminescence lifetime of Er has increased by 1.73 times and 1.50 times, respectively. Thus, it is proved that the nanoshell can insulate the luminescence center from the external interference environment so as to guarantee a long life of the luminescence center. It is worth noting that although the designed dye-sensitized Nd^{3+}-doped nanostructure has a better excitation wavelength near 800 nm, but $NaYF_4$:Yb/Er (20/2%) nanoparticles can only be excited by 980 nm wavelength. As shown in Fig. 4(b), the exicitation wavelength was 980 nm, not the conventional 808 nm wavelengh. Furthermore, the Fig. 4(c) shows that the luminescence life of CSS nanostructure remains unchanged whether dye molecules are connected or not. This further proves that the nanoshell can effectively prevent the interaction between the luminescence center and the external environment, thus enhancing the up-conversion luminescence

The difference of Nd^{3+} sensitization system lies in the fact that its outermost nanoshell is doped with only Nd^{3+} ions, rather than the previously reported Nd-Yb ions[16]. This structural design is based on the results of our experiments. As shown in Fig. 5, with the increase of Yb^{3+}-doping concentration in the outermost layer, the up-conversion luminescence intensity of dye-sensitized CSS structure will gradually decrease. According to our previous research of dye-sensitized rare earth up-conversion nanosystem, the excitation energy absorbed by dye needs to be gradually transferred to the internal luminescence center[17]. In this process, the energy loss in the migration of excitation energy to the surface is very heavy. The doped Yb^{3+} ions are likely to transfer the excitation energy to the surface[9, 23-24], thus reducing the excitation energy transferred to the interior and weakening the up-conversion luminescence. Therefore, the strongest dye-sensitized up-conversion luminescence is produced in the outermost nanoshell

without doped Yb^{3+} ions, as shown in Fig. 5.

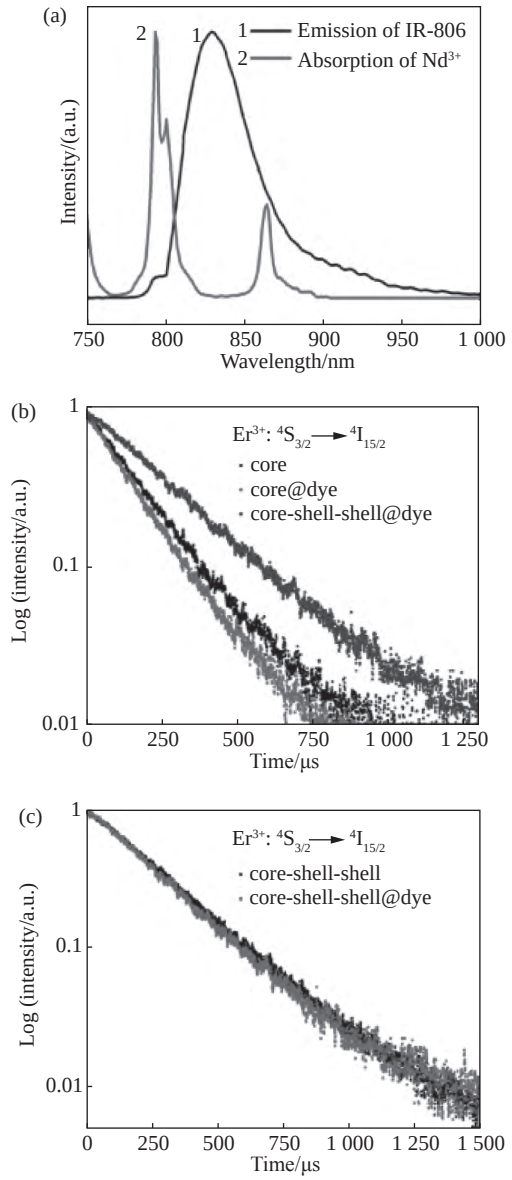

Fig. 4 (a) Overlap between the emission spectrum of IR-806 molecules and the absorption spectrum of Nd^{3+}; (b) the lifetimes of Er^{3+} ($^4S_{3/2}\rightarrow{}^4I_{15/2}$) in core nanoparticles (black, $NaYF_4$:Yb/Er (20/2%), dye-sensitized core nanoparticles (red) and dye-sensitized CSS nanostructure (blue) under 980 nm excitation; (c) the lifetimes of Er^{3+} ($^4S_{3/2}\rightarrow{}^4I_{15/2}$) in CSS nanostructure and dye-sensitized CSS nanostructure under 808 nm excitation

图 4 (a) IR-806 分子的发射光谱与 Nd^{3+}的吸收交叠图; (b) 980 nm 激发下, 测试得到的核纳米粒子(黑色, $NaYF_4$: Yb/Er (20/2%)), 染料敏化核纳米粒子(红色)及染料敏化的 CSS 纳米结构(蓝色)的 Er^{3+} ($^4S_{3/2}\rightarrow{}^4I_{15/2}$) 的寿命测试结果; (c) 808 nm 激发下 CSS 纳米结构及染料敏化的 CSS 纳米结构的 Er^{3+} ($^4S_{3/2}\rightarrow{}^4I_{15/2}$) 的寿命测试结果

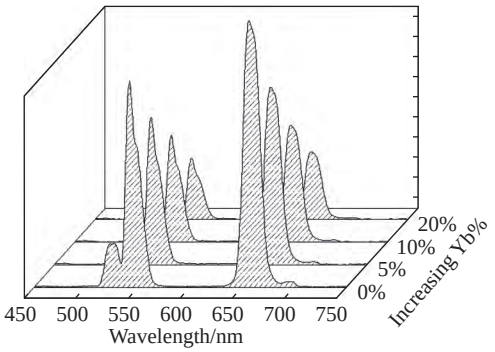

Fig. 5 Upconversion spectra of dye-sensitized $NaYF_4$:Yb/Er (20/2%)@ $NaYF_4$:Yb (10%)@ $NaYF_4$:Nd/Yb (80/*x*%) (*x*=0, 5, 10, 20) nanoparticles under 808 nm excitation

图 5 染料敏化的 $NaYF_4$:Yb/Er (20/2%)@ $NaYF_4$:Yb (10%)@ $NaYF_4$:Nd/Yb (80/*x*%) (*x*=0, 5, 10, 20) 的上转换光谱(808 nm 激发)

3.3 Enhancement of dye-sensitized luminescence by using Ho or Tm as luminescence center

Furthermore, the replacement of luminescence center in the core of CSS structure by Ho ($NaYF_4$: Yb/Ho (20/1%))@ $NaYF_4$:Yb (10%)@ $NaYF_4$:Nd (80%)) or Tm ($NaYF_4$:Yb/Tm (20/1%)@ $NaYF_4$:Yb (10%)@ $NaYF_4$:Nd (80%)) also realized the enhancement of dye-sensitized up-conversion luminescence (Fig. 6 (a) and 6(b), Color online). When the luminescence center was Ho or Tm, the typical nonlinear dependence of luminescence intensity on excitation light power was also shown (Fig. 6(c) and 6(d), Color online). When the luminescence center was Ho, the multi-photon indexes were 1.57 (540 nm emission, $^4S_{13/2}\rightarrow{}^4I_{15/2}$) and 1.88 (645 nm emission, $^4F_{9/2}\rightarrow{}^4I_{15/2}$) respectively. When the luminescence center was Tm, the multi-photon indexes were 2.82 (450 nm emission, $^1D_2\rightarrow{}^3F_4$), 1.74 (470 nm emission, $^1G_4\rightarrow{}^3H_6$), 1.80 (645 nm emission, $^1G_4\rightarrow{}^3F_4$) and 1.34 (695 nm emission, $^3F_2\rightarrow{}^3H_6$) respectively. It should be noted that, for Tm ions, the dye-sensitized up-conversion luminescence had hardly been seen in the $NaYF_4$:Yb/Tm (20/1%) nano-core structure. This is because the 800 nm emission level ($^3H_4\rightarrow{}^3H_6$) of Tm heavily overlapped with the absorption of IR-806 molecules, thus quenching the

Tm luminescence. However, the outer shell of CSS structure successfully blocked the transfer of Tm to IR-806, thus realizing the dye-sensitized up-conversion luminescence.

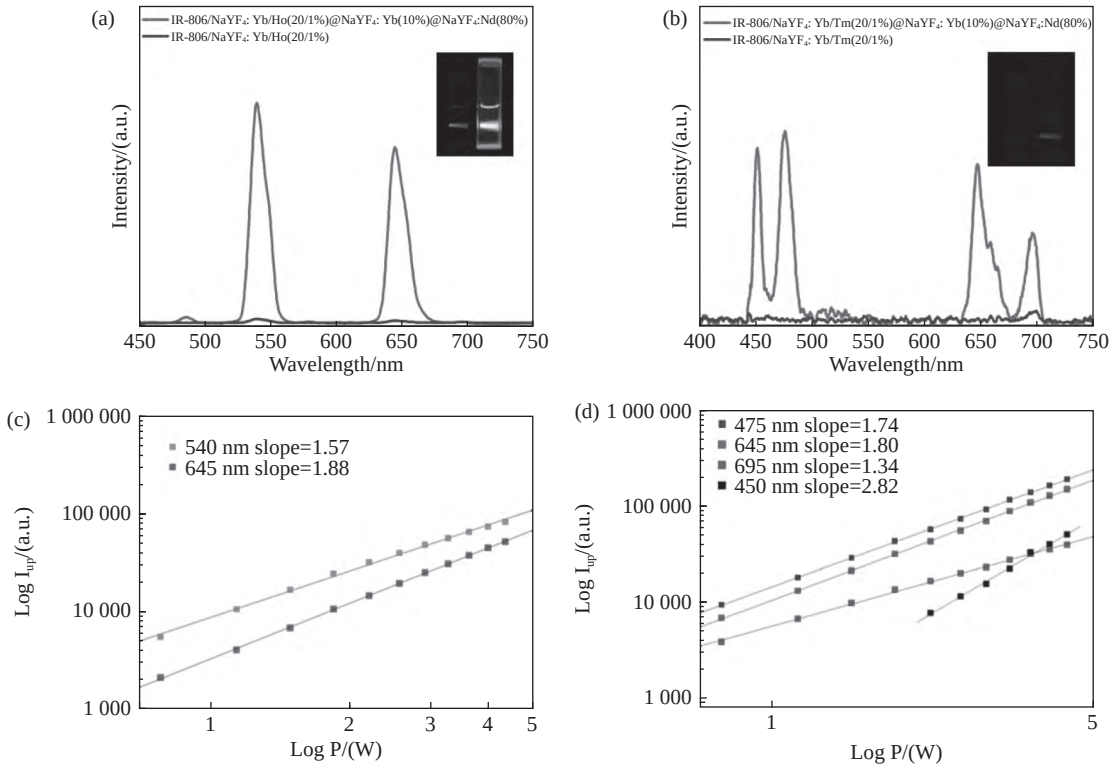

Fig. 6　(a) The UCL of the IR-806 sensitized Ho core nanostructure and IR-806 sensitized Ho-CSS nanostructure, (b) the UCL of the IR-806 sensitized Tm core nanostructure and IR-806 sensitized Tm-CSS nanostructure, (c) log-log plots of the UCL intensity over laser power for the green and red emissions of the dye-sensitized Ho-CSS under 808 nm excitation, (d) log-log plots of the UCL intensity versus laser power for the green and red emissions of the dye-sensitized Tm-CSS under 808 nm excitation

图 6　(a)IR-806 敏化 Ho 核结构及 IR-806 敏化 Ho-CSS 结构的上转换光谱,(b) IR-806 敏化 Tm 核结构及 IR-806 敏化 Tm-CSS 结构的上转换光谱,(c) 808 nm 激发下的 IR-806 敏化的 Ho-CSS 结构的上转换发光强度随功率变化的 log-log 关系,(d) 808 nm 激发下的 IR-806 敏化的 Tm-CSS 结构的上转换发光强度随功率变化的 log-log 关系

4　Conclusion

Highly uniform $NaYF_4$:Yb/Er (20/2%)@ $NaYF_4$:Yb (10%)@ $NaYF_4$:Nd (80%) up-conversion nanoparticles were successfully prepared. Their up-conversion luminescence intensity was about 38 times stronger than that of dye-sensitized $NaYF_4$: Yb/Er (20/2%) core nanostructure. Further studies showed that there were two reasons for this enhancement. On the one hand, the heavy overlap between the Nd absorption in the outmost layer and the emission of dye IR-806 molecules led to the effective absorption of the excitation energy of dye. On the other hand, due to the protective effect of nanoshell layer on the luminescence center, the luminescence life of this structure was 1.73 times longer than that of dye-sensitized core nanostructure. By changing the doping concentration of Yb^{3+} ions in the outermost layer, we demonstrated that the dye-sensitized up-conversion luminescence would be weakened by the doping of Yb^{3+} ions, and could become the strongest without the doping of Yb^{3+} ions. Furthermore, this dye-sensitized CSS structure has realized the enhancement of dye-sensitized up-conversion luminescence intensity when the luminescence center is Ho or Tm.

——中文对照版——

1 引 言

稀土离子由于其具有 4f 电子组态内及 4f 到 5d 之间的电子跃迁的特异性，导致其可产生从紫外、可见光区到红外光区的多种波长的光子辐射[1-2]。尤其是，稀土离子掺杂的上转换纳米粒子 (UCNPs) 具备将两个及两个以上的低能量近红外光子转换为一个高能量光子的特性，其产生的光子发射具有谱带窄、抗漂白、背景噪声低等优点[3]。这种近红外光激发的上转换发光特性将产生诸多应用，如超分辨成像、荧光标记、光动力治疗、光学防伪等[4-8]。

尽管稀土离子掺杂产生的上转换发光有诸多应用，但其相对较低的发光强度限制了其进一步实际应用。如何增强上转换发光一直是上转换发光研究中亟待解决的问题。近年来，如核壳纳米结构[9]、等离子体场增强发光[10]、染料敏化发光[11]，实现了上转换发光强度的增强。特别是，染料敏化发光的研究不仅增强了上转换发光的强度，也拓宽了上转换发光的激发范围。相对于吸收弱的稀土离子 (吸收系数为 0.1~10 M^{-1} cm^{-1})，改用近红外染料 (吸收系数为 1 000 ~10 000 M^{-1} cm^{-1}) 来吸收近红外光可实现敏化增强上转换发光。然而，大部分近红外染料发射波长 (800~900 nm) 和经典的 Yb 敏化掺杂体系的 Yb 的吸收波长（950~1 000 nm）的交叠积分较小，从而限制了染料敏化上转换发光的增强。进一步，设计采用 Nd 和 Er 离子敏化体系作为染料敏化的受主[12-13]，实现更有效的染料敏化上转换发光的增强。Nd^{3+}敏化上转换发光是近些年发展的上转换发光体系，尤其是其分区掺杂策略可以实现高效的上转换发光[14-16]。目前为止，染料敏化的 Nd 离子掺杂体系通常采用的是 Nd 敏化上转换发光的最佳结构设计。考虑到染料敏化过程中染料会与稀土发光体系相互作用从而减弱发光[17]，因此，设计优化染料敏化增强的 Nd 掺杂的上转换发光体系，将能更有效地应用于生化分析、肿瘤诊疗、发光显示等领域[18-22]。

本文设计采用 Nd 敏化的核/壳/壳结构作为增强染料敏化上转换发光的受主，通过采用高温热分解方法成功制备 Nd 敏化的核/壳/壳结构，并与染料 IR-806 分子耦连实现染料敏化上转换发光强度的增强。相关的结构表征证实纳米结构的有效性。进一步通过发射光谱，荧光寿命光谱分析等研究了其背后的增强机制。通过优化最外层壳中 Yb 离子的掺杂浓度，证实无 Yb 掺杂情况下染料敏化上转换发光最强。

2 实 验

2.1 实验原料

氯化镱 ($YbCl_3·6H_2O$ (99.99%)、氯化钇（$YCl_3·6H_2O$）、氯化铒（$ErCl_3·6H_2O$）、氢氧化钠（NaOH, 98%）、氟化铵（NHF_4, 99.99%）、IR-780 iodide (99%)、4-巯基苯甲酸 (99%)、1-十八烯 (ODE)、油胺 (90%)(OM) 和油酸 (90%)(OA)，购于 Sigma-Aldrich 公司。根据参考文献 [14]，Nd ($CF_3COO)_3$ 通过将 Nd_2O_3 粉末与过量的三氟醋酸反应，然后蒸发除去过量的三氟醋酸获得。三氟醋酸镱 ($Yb(CF_3COO)_3$)、三氟醋酸钇 ($Y(CF_3COO)_3$)、三氟醋酸钠 (CF_3COONa) 购于 GFS Chemicals。二氯甲烷及三氯甲烷、二甲基甲酰胺 (DMF) 购买于北京化工厂。所有的化学试剂都是分析纯度。

2.2 合成上转换纳米粒子

该核壳壳层上转换纳米结构基于已发表的化学方法制备[14-15]。首先，合成核结构，将 $YbCl_3·6H_2O$ (0.1 mmol)，$YCl_3·6H_2O$ (0.39 mmol) 和 $ErCl_3·6H_2O$ (0.01 mmol) 溶解在 3 mL OA, 7.5 mL ODE 的三口瓶中，并加热到 150 ℃，保持 30 min，之后在氩气保护下冷却至室温。然后，配置 NH_4F (2 mmol)，NaOH (1.25 mmol)，使其溶解在 5 mL 甲醇中，并加入到以上稀土盐的三口瓶中，加到 70 ℃ 去除甲醇，再加热到 300 ℃ 并保持 1 h。然后，加入 0.25 mmol $NaYF_4$:Yb (10%) 活性壳在 ODE 中（通过三氟醋酸盐法合成），加热并熟化 10 min。然后加入 0. 5 mmol $NaYF_4$:Nd (20%) 活性壳（通过三氟醋酸盐法合成），并熟化 10 min。最后，使溶液冷却到室温，并使用乙醇离心，将上述混合物溶解

在 6 mL 三氯甲烷中。不同稀土元素掺杂的核壳壳层上转换纳米结构均采用类似方法合成。

2.3　合成 IR-780 分子

根据文献 [11] 方法, 类似地, 在氮气保护下, 将有机 IR-780 分子 (250 mg), 4-巯基苯甲酸 (115.5 mg), 和 DMF (10 mL) 溶解在 50 mL 三口瓶中, 使混合溶液在氮气环境下维持 17 h。产物溶液用 0.45 μm PTFE 过滤后, 减压蒸馏去除 DMF。然后, 将残余物溶解在 5 mL 二氯甲烷中, 再次通过 0.45 μm PTFE 过滤, 并用冰乙醚实施沉淀。最后, 将反应物在真空下过滤、干燥并避光保存。

2.4　合成 IR-806 分子

采用类似于文献 [8, 17] 的方法, 将 1 mL IR-806 (*x* mg/mL, *x* 为 0 ~ 20 mg/mL) 溶解在三氯甲烷中, 并与 1 mL β-$NaYF_4$:Yb/Er(20/2%) @ $NaYF_4$:Yb (10%)@ $NaYF_4$:Nd (20%) 纳米粒子混合, 其中 (Er^{3+} ~1.67 mM)。将得到的反应混合物搅拌 24 h 在室温下离心, 重新分散在 1 mL 三氯甲烷中。对 IR-806 敏化的 UCNPs 进行上转换光谱测试时, 在稀土纳米粒子中的 Er^{3+} 离子浓度约为 16 μM 的条件下进行。

2.5　实验表征测试

透射电镜 (TEM) 测试: 采用 Tecnai G2 F20 S-Twin 电子显微镜在 200 kV 电压下测试。X-ray 衍射 (XRD) 测试通过 Rigaku D/max-2000 完成, 衍射半径采用 Cu Kα radiation (λ=0.154 1 nm)。吸收光谱利用 Maya 2000 光谱仪完成测试 (Ocean optics)。利用外在耦合的 808 nm 激光在海洋光学光谱仪(Maya2000)记录上转换光谱。通过 Hitachi, S-4800 表征能谱(EDS)。上转换发光的荧光寿命测试采用 500 MHz TDS 3052 作为激发光源, 通过 OPO(Sunlite 8000) 及示波器获得荧光寿命数据。

3　实验结果与讨论

3.1　纳米粒子形貌及表征

采用高温热分解法制备高度均匀的 Nd^{3+}敏化核/壳/壳上转换 $NaYF_4$:Yb/Er (20/2%)@ $NaYF_4$:Yb (10%)@ $NaYF_4$:Nd (80%) 纳米核结构。透射电镜照片显示上转换纳米粒子的尺寸均匀。图 1 为上转换纳米粒子的核、核/壳、核/壳/壳电镜表征图及尺寸分布图。由平均粒径大小统计结果可知, 核 ($NaYF_4$:Yb/Er (20/2%), 记为 C), 核/壳 ($NaYF_4$:Yb/Er (20/2%)@ $NaYF_4$:Yb (10%), 记为 CS), 核/壳/壳 ($NaYF_4$:Yb/Er (20/2%)@ $NaYF_4$:Yb (10%)@ $NaYF_4$:Nd (80%)), 记为 CSS) 的平均尺寸分别为 23.5、26.3、33.6 nm。这证实结构存在约 1.4 nm 的 Yb 过渡层, 3.7 nm 的 Nd 敏化纳米壳层逐步生长在 $NaYF_4$:Yb/Er 纳米核上面。图 2(a) 为上转换纳米粒子的核、核/壳、核/壳/壳 XRD 图, 显示合成的 UCNPs 为经典的六角相结构 (JCPDS-16-0334), EDS 证实 Nd、Y、Yb 等稀土元素有效地掺杂进纳米粒子内(图 2(b))。进一步, 根据文献的方法(图 2(c)), 合成了 IR-806 分子, 由吸收图(图 2(d))可见, 其吸收峰位从 780 nm 移动到 806 nm, 结果证实成功合成了 IR-806 分子。进一步, 根据前面的方法将 IR-806 分子修饰到上转换纳米粒子表面。由图 2(d)可知, 当 IR-806 分子修饰到 UCNPs 上之后, 其吸收峰位被 IR-806 的吸收所掩盖, 从而证实染料分子成功修饰到 UCNPs 上。

3.2　染料敏化增强机制证实与讨论

相对于最早报道的经典的 IR-806 敏化 $NaYF_4$:Yb/Er (20/2%) 纳米粒子[11], 本文设计的染料敏化 CSS 结构的上转换发光强度 (图 3(a)) 增强了约 38 倍。证实本文设计的染料敏化结构实现了上转换发光强度的增强。另外, 在近红外 (808 nm) 光激发下, 染料敏化 CSS 结构的上转换红光发射与绿光发射均表现出发光强度随激发光功率的非线性依赖特性(图 3(b)), 其多光子指数分别为 1.67(绿光 540 nm发射 $^4S_{13/2}\rightarrow{}^4I_{15/2}$), 2.0(红光 655 nm 发射$^4F_{9/2}\rightarrow{}^4I_{15/2}$), 证实其发光特性为非线性的上转换发光。

本文设计的染料敏化 CSS 结构的上转换发光强度相对于染料敏化的核纳米粒子增强约 38 倍。对于这种增强, 分析认为: 一方面, 在 CSS 纳米结构中最外层为 Nd^{3+}离子掺杂壳层, 而由图 4(a)(彩图见期刊电子版)可知, Nd 的吸收与 IR-806 染料分子的发射有大量交叠, 因而, 能够被 IR-806 分子高效敏化; 另一方面, CSS 结构中的纳米壳层可以有效保护发光中心。由图 4(b)(彩图见期刊电子版)可见, 经染料敏化的具有 CSS 结构的 Er 的发光寿命 (253 μs) 明显长于染料敏化核纳米粒子 (146 μs) 及核纳米粒子 (169 μs)

Er 的寿命，发光寿命值分别延长了 1.73 倍及 1.50 倍。证实了纳米壳层隔绝了发光中心与外部环境干扰，使得发光中心产生长的发光寿命。值得注意的是，尽管所设计的染料敏化 Nd^{3+}离子掺杂纳米结构较佳的激发波长在 800 nm 附近，但是在研究发光寿命时，$NaYF_4$:Yb/Er(20/2%) 纳米粒子只能在 980 nm 波长处激发。

传统 (20/2%) 核纳米粒子只能被 980 nm 光激发产生上转换发光，因此，图 4(b)的测试激发波长选择为 980 nm 而非通常采用的 808 nm。由图 4(c)可知，对于 CSS 纳米结构，无论是否连接染料分子，其发光寿命均保持不变。进一步证实纳米壳层有效地阻隔了发光中心与外界环境的相互作用，从而增强了上转换发光。

本文 Nd^{3+}敏化体系的不同之处在于，其最外层的纳米壳层中仅掺杂了 Nd^{3+}，而没有像以往文献报道的将 Nd-Yb 共掺杂到纳米壳层中[16]。这种结构设计是根据实验结果所得。本文所设计的钕敏化多层壳纳米结构的上转换光谱如图 5 所示。可见，随着最外层 Yb^{3+} 掺杂浓度的增加，染料敏化 CSS 结构的上转换发光强度反而逐渐减弱。根据前面的研究可知，染料敏化稀土上转换纳米体系中，染料吸收的激发能需要逐步传递到内部的发光中心[17]，而激发能传递过程中，能量损耗非常大，掺杂 Yb^{3+}离子极易将激发能传递到表面[9, 23-24]，从而使传递到内部的激发能降低，最终导致上转换发光降低。由此可知，最外层的纳米壳层在不掺杂 Yb^{3+}离子的情况下，产生的染料敏化上转换发光最强。

3.3 发光中心为 Ho 及 Tm 时染料敏化发光增强

进一步，对于 CSS 结构，将核内的发光中心换为 Ho ($NaYF_4$:Yb/Ho (20/1%))@ $NaYF_4$:Yb (10%)@ $NaYF_4$:Nd (80%)) 或 Tm ($NaYF_4$:Yb/Tm (20/1%)@ $NaYF_4$:Yb (10%)@ $NaYF_4$:Nd (80%))，同样实现了染料敏化上转换发光的增强(图 6(a)和 6(b)，彩图见期刊电子版)。对于发光中心为 Ho 及 Tm，发光强度同样随激发光功率呈非线性的依赖关系(图 6(c)和 6(d)，彩图见期刊电子版)。对于发光中心为 Ho 的情况，其多光子指数分别为 1.57(540 nm发射 $^4S_{13/2}\rightarrow{}^4I_{15/2}$)，1.88(645 nm 发射$^4F_{9/2}\rightarrow{}^4I_{15/2}$)。对于发光中心为 Tm 的情况，其多光子指数分别为 2.82(450 nm 发射 $^1D_2\rightarrow{}^3F_4$)、1.74(470 nm 发射$^1G_4\rightarrow{}^3H_6$)、1.80(645 nm 发射$^1G_4\rightarrow{}^3F_4$)、1.34(695 nm发射$^3F_2\rightarrow{}^3H_6$)。值得注意的是，对于 Tm 离子，$NaYF_4$:Yb/Tm (20/1%) 纳米核结构，几乎没有染料敏化的上转换发光出现。这是由于 Tm 的 800 nm 发射能级($^3H_4\rightarrow{}^3H_6$)与 IR-806 分子的吸收交叠严重，从而猝灭了 Tm 的发光。而 CSS 结构使得外面的壳层成功地阻隔了 Tm 向 IR-806 传递，从而实现了染料敏化上转换发光。

4 结 论

本文成功制备了高度均匀的 $NaYF_4$:Yb/Er (20/2%)@ $NaYF_4$:Yb (10%)@ $NaYF_4$:Nd (80%) 上转换纳米粒子，其染料敏化上转换发光强度相对于染料敏化的 $NaYF_4$:Yb/Er (20/2%) 核纳米结构增强了约 38 倍。进一步研究表明，这种增强一方面源自最外层 Nd 吸收与染料 IR-806 分子的发射交叠大，导致其能有效吸收染料的激发能。另一方面源自纳米壳层对发光中心的保护作用，相对于染料敏化的核纳米结构，其发光寿命延长了 1.73 倍。通过改变最外层 Yb^{3+}的掺杂浓度，证实掺杂 Yb^{3+}将导致染料敏化上转换发光减弱，而无掺杂 Yb^{3+}的条件下上转换发光最强。最终，采用这种染料敏化的 CSS 结构实现了发光中心为 Ho 及 Tm 的染料敏化上转换发光强度的增强。

参考文献：

[1] AUZEL F. Upconversion and anti-stokes processes with f and d ions in solids[J]. *Chemical Reviews*, 2004, 104(1): 139-174.

[2] 李晓晓, 李蕴乾, 汪欣, 等. 高灵敏度下转换光学测温材料: $NaGd(WO_4)_2$:Yb^{3+}/Er^{3+}[J]. 中国光学, 2019, 12(3): 596-605.
LI X X, LI Y Q, WANG X, *et al*.. Highly sensitive down-conversion optical temperature-measurement material: $NaGd(WO_4)_2$:Yb^{3+}/Er^{3+}[J]. *Chinese Optics*, 2019, 12(3): 596-605. (in Chinese)

[3] 贺飞, 盖世丽, 杨飘萍, 等. 稀土上转换荧光材料的发光性质调变及其应用[J]. 发光学报, 2018, 39(1): 92-106.

HE F, GAI SH L, YANG P P, *et al*.. Luminescence modification and application of the lanthanide upconversion fluorescence materials[J]. *Chinese Journal of Luminescence*, 2018, 39(1): 92-106. (in Chinese)

[4] WANG F, WEN SH H, HE H, *et al*.. Microscopic inspection and tracking of single upconversion nanoparticles in living cells[J]. *Light*: *Science & Applications*, 2018, 7(4): e18007.

[5] CHEN SH, WEITEMIER A Z, ZENG X, *et al*.. Near-infrared deep brain stimulation via upconversion nanoparticle-mediated optogenetics[J]. *Science*, 2018, 359(6376): 679-684.

[6] LIU Y J, LU Y Q, YANG X S, *et al*.. Amplified stimulated emission in upconversion nanoparticles for super-resolution nanoscopy[J]. *Nature*, 2017, 543(7644): 229-233.

[7] WANG D, XUE B, OHULCHANSKYY T Y, *et al*.. Inhibiting tumor oxygen metabolism and simultaneously generating oxygen by intelligent upconversion nanotherapeutics for enhanced photodynamic therapy[J]. *Biomaterials*, 2020, 251: 120088.

[8] XUE B, WANG D, ZHANG Y L, *et al*.. Regulating the color output and simultaneously enhancing the intensity of upconversion nanoparticles via a dye sensitization strategy[J]. *Journal of Materials Chemistry C*, 2019, 7(28): 8607-8615.

[9] TU L P, LIU X M, WU F, *et al*.. Excitation energy migration dynamics in upconversion nanomaterials[J]. *Chemical Society Reviews*, 2015, 44(6): 1331-1345.

[10] 徐文, 陈旭, 宋宏伟. 稀土离子上转换发光中的局域电磁场调控[J]. 发光学报, 2018, 39(1): 1-26.
XU W, CHEN X, SONG H W. Manipulation of local electromagnetic field in upconversion luminescence of rare earth ions[J]. *Chinese Journal of Luminescence*, 2018, 39(1): 1-26. (in Chinese)

[11] ZOU W Q, VISSER C, MADURO J A, *et al*.. Broadband dye-sensitized upconversion of near-infrared light[J]. *Nature Photonics*, 2012, 6(8): 560-564.

[12] CHEN G Y, DAMASCO J, QIU H L, *et al*.. Energy-cascaded upconversion in an organic dye-sensitized core/shell fluoride nanocrystal[J]. *Nano Letters*, 2015, 15(11): 7400-7407.

[13] WANG D, WANG D, KUZMIN A, *et al*.. ICG-sensitized $NaYF_4$:Er nanostructure for theranostics[J]. *Advanced Optical Materials*, 2018, 6(12): 1701142.

[14] WANG D, XUE B, KONG X G, *et al*.. 808 nm driven Nd^{3+}-sensitized upconversion nanostructures for photodynamic therapy and simultaneous fluorescence imaging[J]. *Nanoscale*, 2015, 7(1): 190-197.

[15] WANG D, XUE B, SONG J, *et al*.. Compressed energy transfer distance for remarkable enhancement of the luminescence of Nd^{3+}-sensitized upconversion nanoparticles[J]. *Journal of Materials Chemistry C*, 2018, 6(24): 6597-6604.

[16] ZHONG Y T, TIAN G, GU Z J, *et al*.. Elimination of photon quenching by a transition layer to fabricate a quenching-shield sandwich structure for 800 nm excited upconversion luminescence of Nd^{3+} -sensitized nanoparticles[J]. *Advanced Materials*, 2014, 26(18): 2831-2837.

[17] XUE B, WANG D, TU L P, *et al*.. Ultrastrong absorption meets ultraweak absorption: unraveling the energy-dissipative routes for dye-sensitized upconversion luminescence[J]. *Journal of Physical Chemistry Letters*, 2018, 9(16): 4625-4631.

[18] 李晶, 刘璐, 郭会琴, 等. 基于氟-氟相互作用的上转换荧光法快速测定水中的全氟辛烷磺酸[J]. 分析化学, 2019, 47(3): 380-387.
LI J, LIU L, GUO H Q, *et al*.. An upconversion fluorescent method for rapid detection of perfluorooctane sulfonate in water samples based on fluorine- fluorine interaction[J]. *Chinese Journal of Analytical Chemistry*, 2019, 47(3): 380-387. (in Chinese)

[19] 邵帅, 丁彬彬, 朱忠丽, 等. 利用主客体化学制备水溶性上转换纳米药物及在肿瘤诊疗中的应用[J]. 分析化学, 2019, 47(6): 823-831.
SHAO SH, DING B B, ZHU ZH L, *et al*.. Preparation of water-soluble up-conversion nano-drug by host-guest chemistry and its application in tumor diagnosis and treatment[J]. *Chinese Journal of Analytical Chemistry*, 2019, 47(6): 823-831. (in Chinese)

[20] 崔琳, 赵敏惠, 张春阳. 主客体作用在生化分析中的应用研究进展[J]. 分析化学, 2020, 48(7): 817-826.
CUI L, ZHAO M H, ZHANG CH Y. Recent advance in applications of host-guest interaction in biochemical analysis[J]. *Chinese Journal of Analytical Chemistry*, 2020, 48(7): 817-826. (in Chinese)

[21] 孟志鹏, 武素丽. 光子晶体对稀土上转换发光的调控[J]. 发光学报, 2020, 41(8): 913-925.
MENG ZH P, WU S L. Manipulating upconversion luminescence of rare earth by photonic crystals[J]. *Chinese Journal of Luminescence*, 2020, 41(8): 913-925. (in Chinese)

[22] 孙剑飞, 闫东, 刘禄. 单颗粒稀土纳米晶的三基色上转换发光[J]. 发光学报, 2020, 41(1): 1-8.
SUN J F, YAN D, LIU L. Three-primary-color upconversion in single lanthanide based nanoparticle[J]. *Chinese Journal of Luminescence*, 2020, 41(1): 1-8. (in Chinese)

[23] 于海洋, 涂浪平, 张友林, 等. 溶剂中稀土上转换纳米粒子表面猝灭效应的定量分析[J]. 中国光学, 2019, 12(6): 1288-1294.
YU H Y, TU L P, ZHANG Y L, *et al*.. Quantitative analysis of the surface quenching effect of lanthanide-doped upconversion nanoparticles in solvents[J]. *Chinese Optics*, 2019, 12(6): 1288-1294. (in Chinese)

[24] FISCHER S, BRONSTEIN N D, SWABECK J K, *et al*.. Precise tuning of surface quenching for luminescence enhancement in core-shell lanthanide-doped nanocrystals[J]. *Nano Letters*, 2016, 16(11): 7241-7247.

Author Biographics:

WANG Dan (1986—), female, born in Songyuan City, Jilin province. She is a doctor and postdoctor. In 2015, she received her doctorate from the Changchun Institute of Optics, Fine Mechanics and Physics, Chinese Academy of Sciences. She is mainly engaged in the design of luminescent materials, the bio-functionalization of nanomaterials, and the application of biological photonics and nano-biomedicine. E-mail: wangdan66322@163.com

王 丹(1986—), 女, 吉林松原人, 博士, 2015 年于中国科学院长春光学精密机械与物理研究所获得博士学位, 主要从事发光材料设计, 纳米材料生物功能化, 生物光子学及纳米生物医学应用方面的研究。E-mail: wangdan66322@163.com

KONG Xiang-gui (1955—), male, born in Qufu City, Shandong Province. He is a doctor, researcher and doctoral supervisor. He received his bachelor's degree from the University of Science and Technology of China in 1980 and his doctor's degree from the Changchun Institute of Optics, Fine Mechanics and Physics, Chinese Academy of Sciences in 1998. He is currently a director of the Biophysical Society of China, mainly engaged in the research on the application of biomedical imaging, photodynamic therapy and luminescent nanomaterials in biomedicine. E-mail: xgkong14@ciomp.ac.cn

孔祥贵(1955—), 男, 山东曲阜人, 博士, 研究员, 博士生导师, 1980 年于中国科学技术大学获得学士学位, 1998 年于中国科学院长春光学精密机械与物理研究所获得博士学位, 现任中国生物物理学会理事, 主要从事生物医学成像, 光动力治疗, 发光纳米材料在生物医学中的应用研究。E-mail: xgkong14@ciomp.ac.cn